SUPPLEMENTARY DATA

Supplementary Table 1. Sampling parameters for the morphometrical analyses

Time (post-DT)	**Control mice** (age-matched)				**DT-treated mice**			
	mice	pancreatic surface (mm^2)	α-cells scored	islets scored	mice	pancreatic surface (mm^2)	α-cells scored	islets scored
1 week	3	694.71	4873	677	3	696.80	**98**	771
1 month	3	634.58	7711	731	3	709.58	**129**	775
6 months	4	1026.30	10024	1424	4	1154.38	**401**	1553

Supplementary Table 2. Pancreatic and Plasma Glucagon (2-month-old male mice; 1 week post-DT)

	Control				**DT-treated**						
	mean	sem		n	mean		sem		n	% of control	fold change
Total pancreatic glucagon content (ng)	746.6	±	45.5	10	**7.3**	***	±	0.5	6	0.98	-101.7
Body weight (g)	28.6	±	1.0	3	26.8	**ns**	±	0.7	4	93.68	-1.1
Observed plasma glucagon (pg/ml)	59.3	±	4.5	14	**38.7**	***	±	1.2	10	65.24	-1.5
Estimated total plasma volume (3.7% of body weight [§])	1.1	ml			1.0		ml				
Estimated plasma glucagon (pg/ml) if all pancreatic glucagon were released into circulation	704709				**7395**						

SUPPLEMENTARY DATA

Supplementary Figure 1. DT-mediated cell ablation is specific to pancreatic α-cells in *Glucagon-DTR* mice. Pancreatic somatostatin-expressing δ-cells, insulin-expressing β-cells and pancreatic polypeptide (PP)-producing PP-cells are still present after DT administration. Only glucagon-expressing α-cells are eliminated. Scale bars: 20 μm.

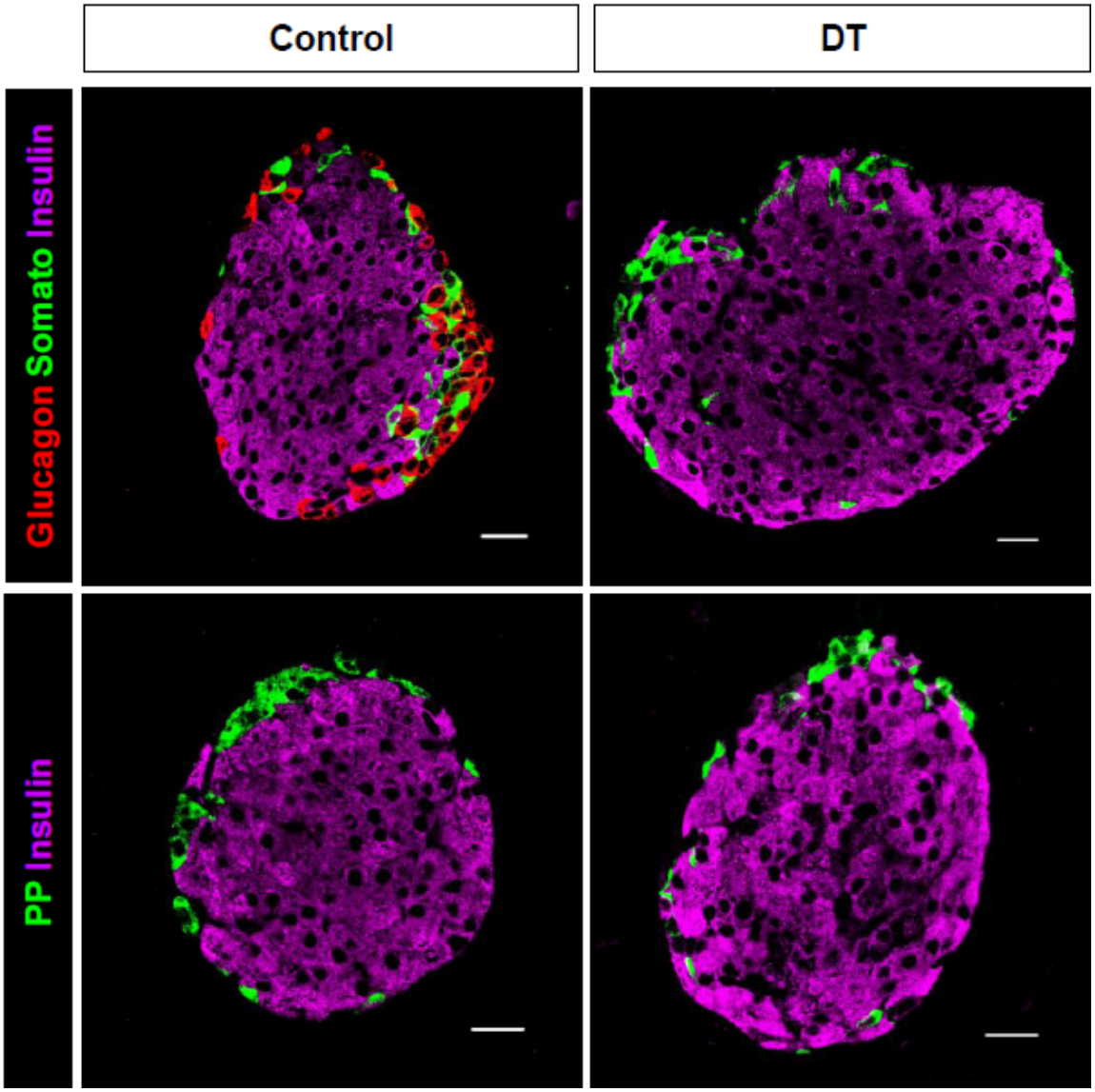

SUPPLEMENTARY DATA

Supplementary Figure 2. Glucagon protein is not produced by intestinal cells after α-cell ablation in *Glucagon-DTR* mice. **A**, Intestinal GLP1-expressing L-cells (white arrowheads) are still observed after DT. Note that polyclonal GLP1 antibody labels pancreatic α-cells (yellow staining in an islet, right column), whereas monoclonal Glucagon antibody does not label intestinal GLP1-producing L-cells, thus indicating that glucagon protein is not produced by intestinal cells, even after DT. Scale bars: 20 μm. **B**, Glucagon content in pancreas and intestine, before and after massive α-cell ablation. Pancreatic glucagon levels after DT are just above the limit of detection in *Glucagon-DTR* mice, whereas intestinal glucagon is always at background level, and is not increased after DT. **C**, Plasma active GLP-1 and GIP levels were not significantly changed after DT (control: 147.7±28.4 pg/ml, n=3, and DT: 180.9±11.1 pg/ml, n=3 for active GLP-1; control: 125.4±24.7 pg/ml, n=10, and DT: 119.2±15.8 pg/ml, n=7 for GIP).

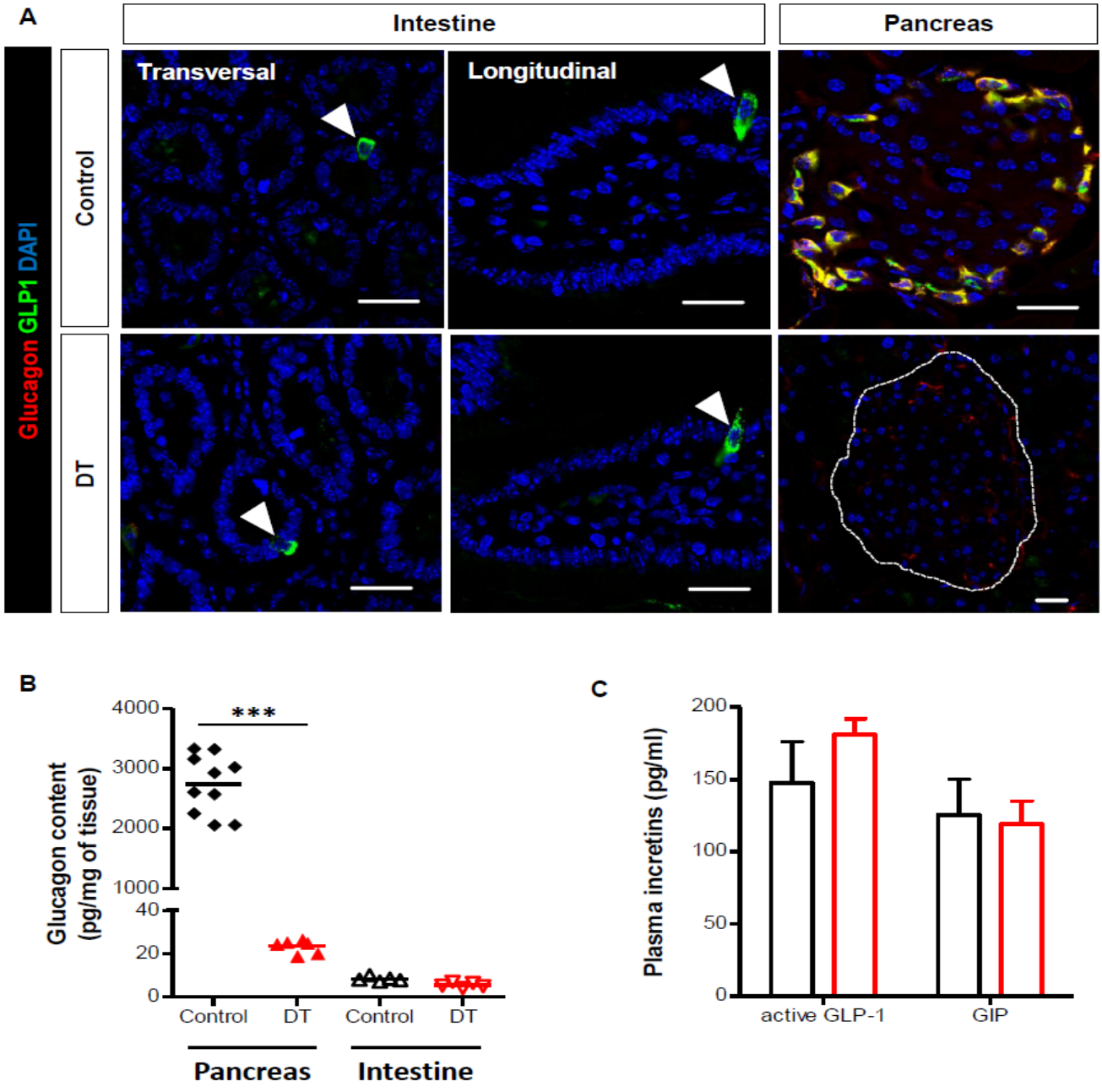

SUPPLEMENTARY DATA

Supplementary Figure 3. Additional Metabolic parameters. A-B, Evolution of body weight (A) and glycemia (B) in random-fed controls (n=3; DT-untreated, black diamonds) and DT-treated (n=3; red triangles) *Glucagon-DTR* mice. No significant change was observed during the period of analysis (up to 6 months after DT). **C**, Glycemia in controls and DT-treated *Glucagon-DTR* mice after a prolonged starvation of 27 hours. No significant difference was observed. **D,** qPCR showing the regulation (fold variation) of G6Pase, PEPCK, GcgR and GP genes at 1 week and 6 months post DT-induced alpha-cell ablation. (black – control non-injected; red – DT-treated; n=3 / group: 1 week after DT and n=8 / group: 6 months after DT). **E-F**, Pyruvate tolerance tests performed 1 week (E) or 6 months (F) after DT in DT-treated mice (n=7 at 1 week and n=4 at 6 months) or controls (n=6 at 1 week and n=4 at 6 months). No significant changes were observed. **G**, Glucagon tolerance test performed 1 week after DT in DT-treated mice (red) or controls (black). The grey area shows the phase of glucose mobilization mediated by exogenous glucagon. **H**, Area under the curve (AUC) of the glucose mobilization phase after glucagon challenge (grey phase in **G**; 215.6±19.8, n=2 for controls and 279.5±13.8, n=4 for DT-treated mice; *p=0.02).

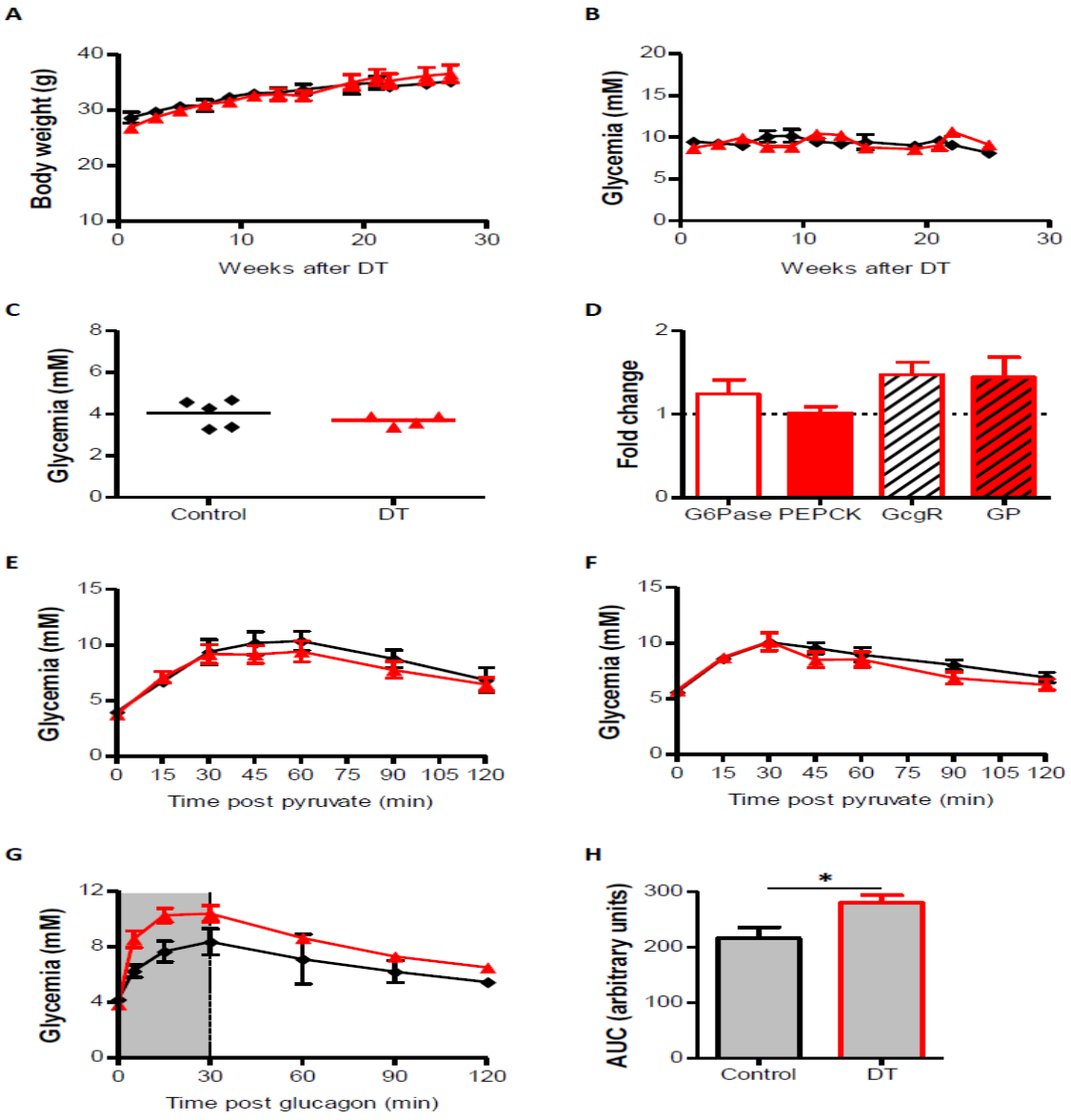

SUPPLEMENTARY DATA

Supplementary Figure 4. DT-treated *Glucagon-DTR* mice are not glucose intolerant 6 months after massive α-cell ablation. Controls: black diamonds, DT-treated *Glucagon-DTR* mice: red triangles (n=4 mice per group).

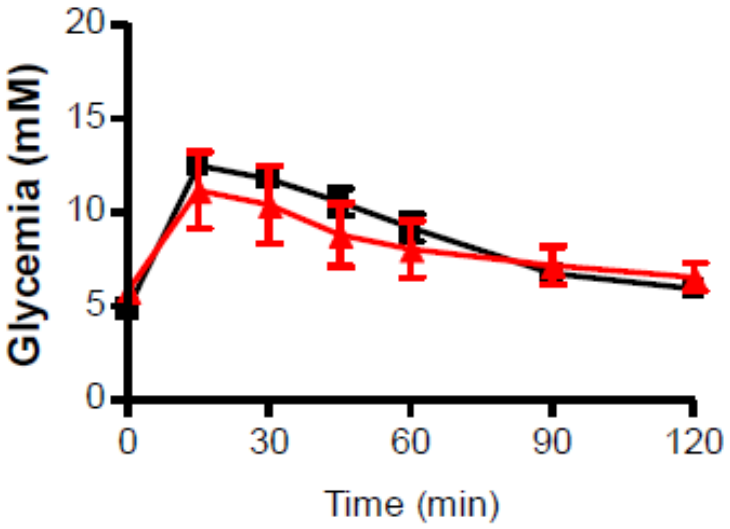

SUPPLEMENTARY DATA

Supplementary Figure 5. Lack of increased α-cell apoptosis after DT in *Glucagon-DTR* mice. **A**, No α-cell death is observed by TUNEL assay in 2 month-old untreated *Glucagon-DTR* mice (controls). **B**, 1 day after DT, many TUNEL+ cells are observed at islet periphery, indicative of massive α-cell death. **B' and B''**: Higher magnification of the square area depicted in **B**. The arrowhead shows a dying cell exhibiting a typical condensed and fragmented pyknotic nucleus. **C-D**, No α-cell death is observed in young adult (2 month-old) or in aged (8 month-old) DT-untreated *Glucagon-DTR* mice (**D**: consecutive pancreatic section of **C**). **C' and D'**: Higher magnification of the area depicted in **C** and **D**, respectively. Numerous α-cells are present (**C'**) at islet periphery, yet no TUNEL+ cell (**D'**) is observed. **E-F**, The very few remaining α-cells after DT are TUNEL- (1 month after DT is shown here). Similar results were observed 1 week or 6 months post DT; **F**: consecutive pancreatic section of **E**). **E' and F'**: Higher magnification of the area depicted in **C** and **D**, respectively. Note that the two α-cells in **E'** are TUNEL- (**F'**) while many TUNEL+ are observed in the adjacent lymph node (LN; internal positive control). Scale bars: **A-B** and **C-F**: 75 μm; **B'** and **B''**: 5 μm.

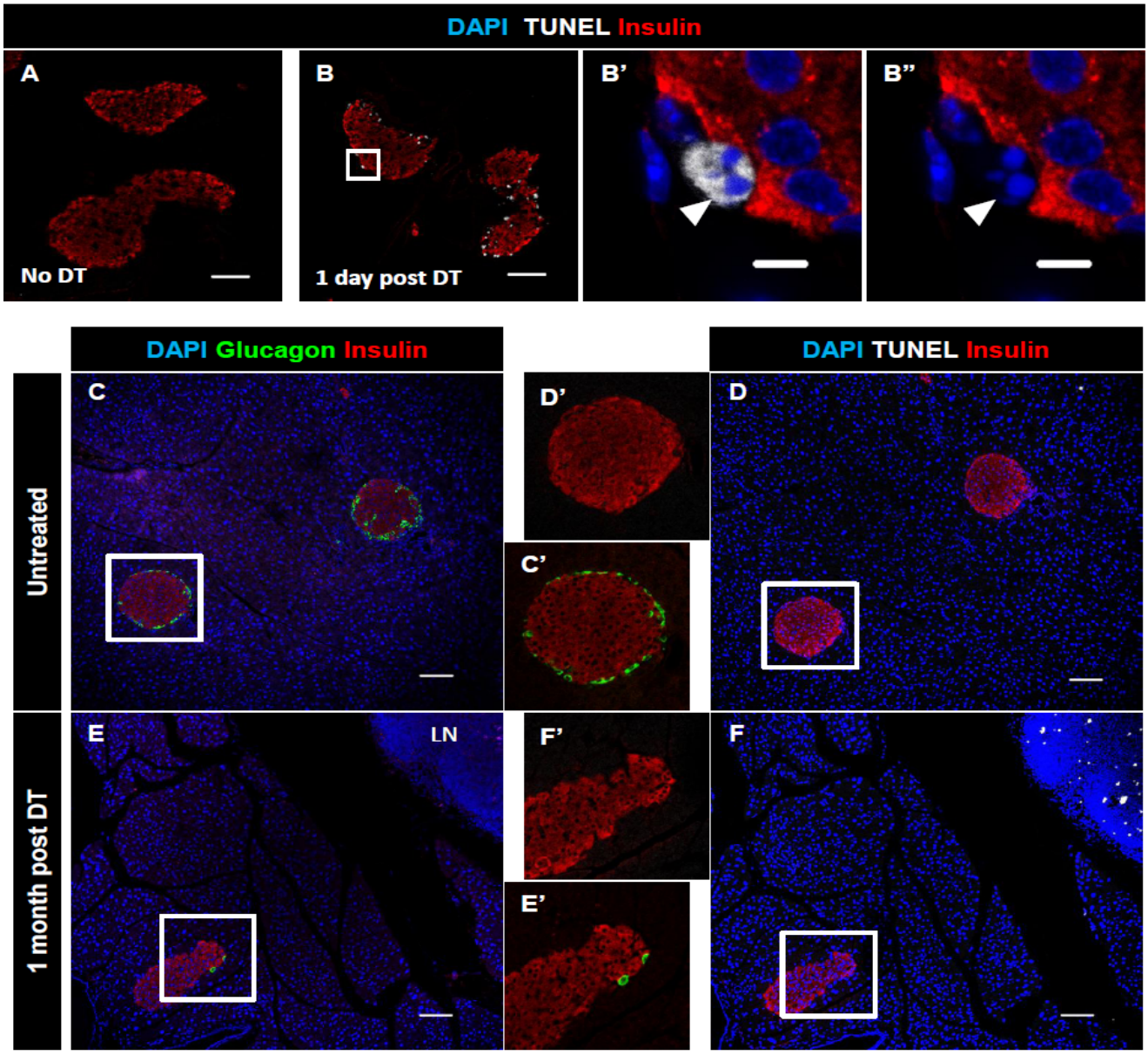

SUPPLEMENTARY DATA

Supplementary Figure 6. Lack of increased α-cell proliferation after DT administration in *Glucagon-DTR* mice. A-B, The mitotic marker phosphohistone H3 (PHH3) stains highly proliferative intestinal cells located in crypts (internal positive control). **C** and **D**, α-cells are not actively proliferating in untreated controls or after DT in *Glucagon-DTR* mice (in **C**, 246 islets were scored, with a total of 4222 glucagon+ cells counted at different ages: only 6 PHH3+ / glucagon+ cells were observed, i.e. 0.14%; in **D,** 1640 islets were scored after 1 week, 1 month and 6 months post DT; among the 522 α-cells observed, only one was PHH3+, i.e. 0.18%). Arrowheads in **C** and **D** indicate non-islet proliferative cells. P: adjacent pancreas tissue. Scale bars: **A**: 75 μm; **B**: 25 μm; **C**-**D**: 20 μm.

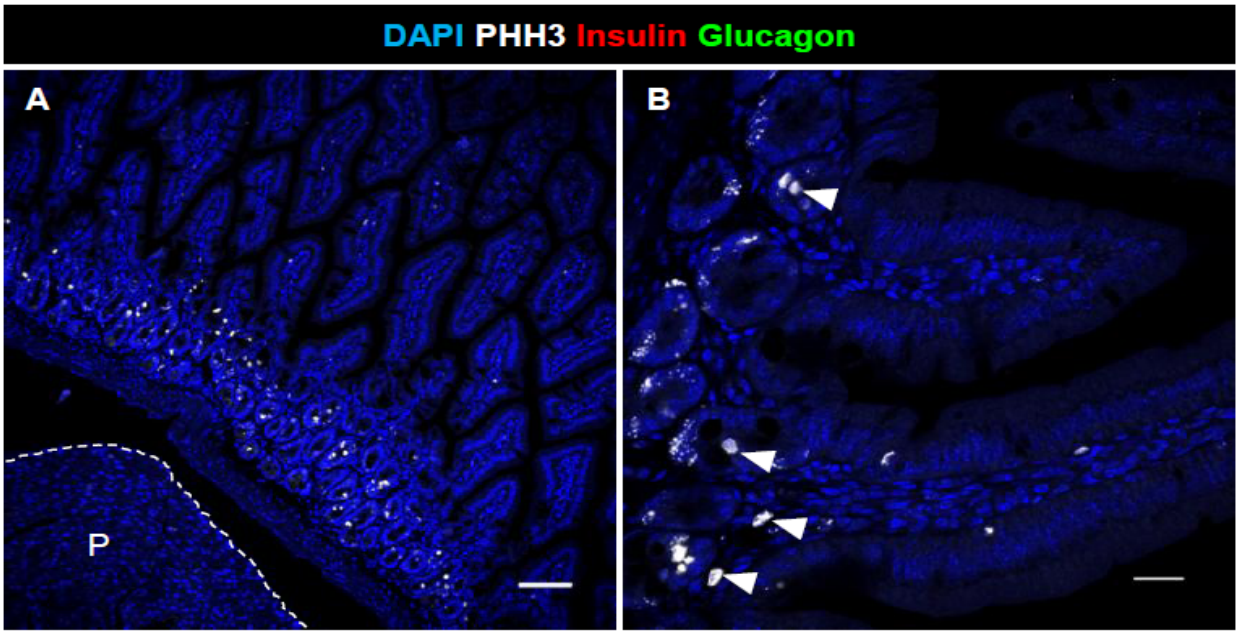

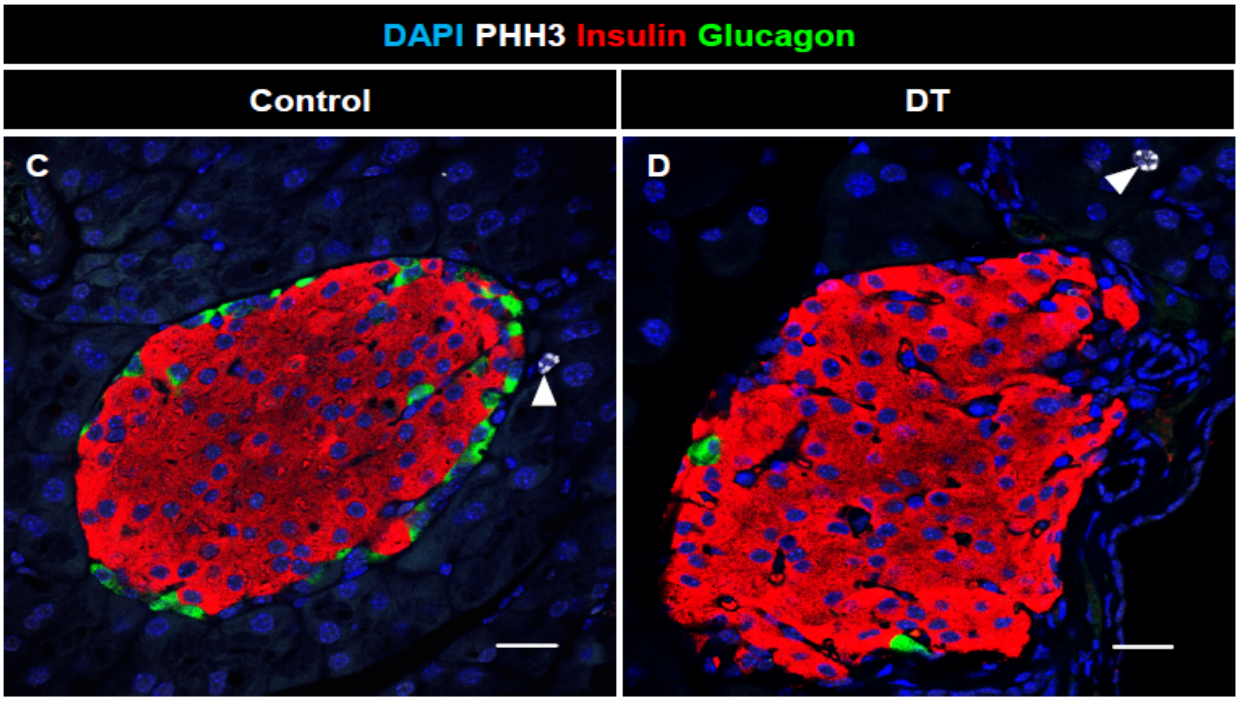

SUPPLEMENTARY DATA

Supplementary Figure 7. Simultaneous α- and β-cell ablation does not prevent DT-induced diabetes. A, Double transgenic mice used. **B**, Experimental design. Transgenic mice were treated with DT and were euthanized 5 days later. Note that DT administration removes >99% of β-cells in *RIP-DTR* mice and animals cannot survive if no exogenous insulin is administered as early as 5 days post-DT. **C-E**, Confocal images of pancreatic sections showing simultaneous DT-mediated α- and β-cell ablation. Arrowhead shows one remaining α-cell after DT. Control represents DT-untreated bitransgenic animals. Scale bars: 20 μm. **F**, Follow up of glycemia. DT-treated doubly transgenics become hyperglycemic after simultaneous α- and β-ablation. By contrast, DT-untreated bitransgenics remain normoglycemic (red triangles: DT-treated double transgenic mice, n=4; black squares: untreated bitransgenic mice, n=4). **G**, Body weights 5 days after DT. Mice treated with DT develop diabetes and become cachectic.